Open Research Online

Multi-photon and electron impact ionisation studies of reactivity in adenine–water clusters

Journal Item

For guidance on citations see FAQs.

Version: Accepted Manuscript

oro.open.ac.uk

Multi-photon and electron impact ionisation studies of reactivity in adenine-water clusters

B. Barc[1], M. Ryszka[1], J.-C. Poully[2], E. Jabbour Al Maalouf[1,3], Z. el Otell[1,3], J. Tabet[3], R. Parajuli[4], P.J.M. van der Burgt[5], P. Limão-Vieira[6], P. Cahillane[1], M. Dampc[1], N.J. Mason[1], S. Eden[1]*

[1] Dept. of Physical Sciences, The Open University, Walton Hall, Milton Keynes, MK7 6AA, United Kingdom

[2] CIMAP/GANIL; Boulevard Henri Becquerel, BP 5133, 14070 Caen cedex 5, France

[3] Dept. of Physics, Faculty of Sciences II, Lebanese University, Fanar – Maten, Lebanon

[4] Dept. of Physics, Amrit Campus, Tribhuvan University, Kathmandu, Nepal

[5] Dept. of Experimental Physics, National University of Ireland Maynooth, Maynooth, Co. Kildare, Ireland

[6] Laboratório de Colisões Atómicas e Moleculares, CEFITEC, Departamento de Física, Faculdade de Ciências e Tecnologia - Universidade Nova de Lisboa, P-2829-516 Caparica, Portugal

* Corresponding author: s.p.eden@open.ac.uk

Abstract

Multi-photon ionisation (MPI) and electron impact ionisation (EII) mass spectrometry experiments have been carried out to probe unimolecular and intermolecular reactivity in hydrated adenine clusters. The effects of clustering with water on fragment ion production from adenine have been studied for the first time. While the observation of NH_4^+ fragments indicated the dissociation of protonated adenine, the dominant hydration effects were enhanced $C_4H_4N_4^+$ production and the suppression of dissociative ionisation pathways with high activation energies. These observations can be attributed to energy removal from the excited adenine radical cation via cluster dissociation. Comparisons of MPI and EII measurements provided the first experimental evidence supporting hypoxanthine formation in adenine-water clusters via theoretically predicted barrierless deamination reactions in closed shell complexes.

1.   Introduction

Radiation induced processes in DNA bases have been investigated intensively in recent years in order to better understand the fundamental process that can initiate DNA lesions [1]. Further interest relates to the mechanisms underpinning the remarkable photo-stability of DNA bases and their possible evolutionary implications. While studies of isolated molecules generally provide the clearest data interpretations, equivalent experiments on hydrogen-bonded complexes enable closer analogies to be drawn with biological environments where different isomeric forms, intermolecular energy transfer processes, and reactivity can be significant. The relaxation pathways of both isolated and hydrated adenine ($C_5H_5N_5$) following excitation to the lowest-lying bright $\pi\pi^*$ state have been mapped out in considerable detail using ultrafast pump-probe experiments [2-4] and quantum chemical calculations [5-7]. Sub-ps-timescale internal conversion to the vibrationally hot electronic ground state via intermediary $n\pi^*$ and $\sigma\pi^*$ states is found to dominate, although evidence for much weaker intersystem crossing pathways to long-lived triplet states has also been reported [8]. Previous studies of reactivity in hydrated adenine have focused on tautomeric transitions [9, 10] and proton transfer in adenine dimer ions [11]. However, no experiments have directly explored the effects of hydration on the dissociative ionisation pathways of adenine. The present work applies UV multi-photon ionisation (MPI) mass spectrometry to analyse fragment ion production from adenine-water clusters. Furthermore, we have carried out the most detailed analysis to date of MPI and electron impact ionisation (EII) production of hydrated adenine monomer ions and hydrated reaction products (notably hydrated protonated adenine) from larger dissociated clusters. The key interest in directly comparing MPI and EII of mixed clusters stems from the selective nature of MPI, notably with water molecule photo-excitation being inaccessible in the present laser conditions.

One possible reaction product of adenine and water that would not be readily identifiable in the mass spectra of hydrated adenine is hypoxanthine ($C_5H_4N_4O$) with mass 136 a.u., equal to protonated adenine or an adenine isotopomer containing one [13]C. The most abundant gas-phase tautomers of adenine (amine-N9H [19]) and hypoxanthine (keto-N1H/N9H [20]) are shown schematically in Fig. 1. A negative activation barrier for hypoxanthine production in the closing system of four water molecules around adenine has been predicted theoretically [12, 13]. While the aim of the present MPI and EII experiments on hypoxanthine is to elucidate adenine-water reactivity, the molecule is also interesting as a *universal* nucleobase that binds without discrimination to natural bases. Its potential applications in polymerase chain reaction (PCR) hybridisation probes and gene therapies have been discussed by Rutledge et al. [14]. In contrast with adenine, very few experimental studies of the photophysical properties of hypoxanthine have been reported in the literature. Electronic spectra and excited state geometries have been investigated theoretically [15], both in isolated and hydrated conditions. As with DNA bases, $\pi\pi^*$ transitions dominate hypoxanthine absorption in the wavelength range (220-225 nm, 5.64-5.51 eV) of the present MPI experiments. Further studies have focused on hydrogen bonding and stacking interactions with DNA bases [14] and gas phase acidity and proton affinity [16].

2. Experimental

The experimental system has been described in a recent publication [17]. Briefly, argon seeded with sublimated adenine or hypoxanthine (Sigma-Aldrich, minimum purity 99%) with or without water vapour flowed continuously through a pinhole (70 μm diameter in the Fig. 1 measurements, 50 μm in Figs. 2 and 3) into a pumped chamber to form a supersonic jet. The argon pressure was varied between 0.5 and 1.8 bar in order to modify the level of clustering in the neutral beam. The highly stable adenine-water clustering conditions required to directly compare MPI and EII mass spectra were achieved by controlling the water and nozzle temperature to within ±1°C using continuous resistive heaters and keeping all parts of the gas line at higher temperatures than the water reservoir. The adenine temperatures (237-276 °C) were comparable with or lower than those applied in previous supersonic beam experiments that reported no evidence for thermally driven decomposition, isomerisation, or reactivity of adenine [18]. The jet passed through a skimmer into a second pumped chamber and crossed an Nd:YAG pumped dye laser beam (*Continuum Powerlight II 8000 - Sirah Cobra-Stretch*, repetition rate 10 Hz, pulse width 7 ns, pulse energy 100-2000 μJ, wavelength 220-277 nm) for MPI measurements or a 200 eV electron beam generated by a commercial gun (*Kimball ELG-2*) for EII experiments. The resulting ions were detected using a reflectron time-of-flight (TOF) mass spectrometer (KORE Technology). The pre-amplified ion signals were timed using a 250 ps resolution *Fast Comtec P7887* time-to-digital conversion (TDC) card. The highest mass resolution we have attained to date was m/Δm = 2,000 using a focused laser beam. The data acquisition system was based on a *LabView* application interfacing with the TDC card and a laser pulse energy meter (*Spectrum Detector SPJ-D-8*). A convex lens on a slider was used to control the laser spot diameter at the interaction with the molecular beam and the average laser pulse energy was adjusted using the delay between the pulses triggering the xenon flash lamps and the *Q-switch* of the Nd:YAG laser.

3. Results and Discussion

3.1. MPI and EII of gas phase adenine and hypoxanthine

Fig. 1 shows MPI and EII production of adenine and hypoxanthine radical cations. The same laser and electron beam conditions were applied for both molecules and the same argon pressure (0.5 bar) was used in all four measurements. Due to its lower vapour pressure, it was necessary to use a higher powder temperature (295°C) for hypoxanthine than for adenine (240°C) to obtain clear signals above background. The mass spectra do not contain peaks for adenine or hypoxanthine clusters ions. While this does not discount the possible presence of clusters in the neutral beams [21], comparisons with previous experiments on adenine suggest that the supersonic expansion conditions were not suitable for significant cluster formation [22]. The ratio of 4±3% for 136 / 135 Th counts in the adenine MPI data is broadly consistent with the ratio of 7.4% expected due to isotopomers [23]. By contrast, Kim et al.'s [24] MPI experiments (ns-timescale pulses at 266 nm) showed a major increase in the 136 / 135 Th

ratio due to intermolecular proton transfer in adenine clusters (discussed further in section 3.2).

Whereas adenine MPI has been observed in the present laser fluence regime in a number of previous studies (222-266 nm) [21, 25-28], the present measurements demonstrate hypoxanthine MPI using ns-timescale laser pulses for the first time. De Vries [29] stated that hypoxanthine can be ionised effectively with 100 fs pulses (wavelength not given) but not with 10 ns pulses. Tembreull and Lubman [25] were unable to ionise hypoxanthine at 222 nm, $\sim 10^6$ Wcm^{-2}. Therefore it is not surprising that the present hypoxanthine MPI signal (220 nm, average fluence 4×10^7 Wcm^{-2}) is relatively weak. Assuming similar EII cross sections for the two molecules at 200 eV (a reasonable expectation according to the binary-encounter-Bethe model [30]), Fig. 1 indicates that adenine MPI is more than six times stronger than hypoxanthine MPI in the present laser conditions. This effect is most likely due to particularly short lifetimes of the electronic excited states of hypoxanthine accessed in the present MPI experiments. Time-resolved experiments are necessary to verify this interpretation and elucidate the relevant excited state dynamics.

3.2.   Hydration effects on fragment ion production from adenine

Fig. 2 compares MPI mass spectra of adenine (A) seeded in argon beams with and without water vapour. The measurements were carried out at relatively low laser fluence (average 4×10^5 Wcm^{-2}, 225 nm) in an effort to reduce cluster dissociation via higher order (≥ 3) photon absorption. The measurement in dry conditions showed a very weak peak for A_2^+ (0.2% of the A^+ signal) and the 136 / 135 Th ratio was 8.0±0.4%, close to the expected isotopomer ratio of 7.4% [23]. This indicates that the adenine molecules were predominantly isolated. The mass spectrum of adenine with water vapour demonstrates $A^+(H_2O)_n$ production up to n=3. It is interesting to note that the intensity of A_2^+ signal is approximately doubled in the hydrated measurement (($9 \pm 2) \times 10^{-3}$ counts / pulse compared with $(4 \pm 1) \times 10^{-3}$ counts / pulse in dry conditions), suggesting that the presence of water in the expansion aids the formation of complexes with two or more adenine molecules.

The hydrated measurement in Fig. 2 shows a 136 / 135 Th ratio of 23±2%, clearly larger that the adenine isotopomer ratio. The extra 136 Th ions can be assigned to AH^+ formation via intermolecular proton transfer and subsequent cluster dissociation. Hünig et al.'s [11] time-dependent pump-probe experiments on pure adenine complexes demonstrated that AH^+ fragment ions were produced by proton transfer in adenine dimer ions. Indeed, proton transfer from A^+ to A in a dimer cation is exothermic: the proton affinity of neutral adenine is 9.78 eV [31] while the acidity of the adenine radical cation is 9.58 eV [32]. Park et al.'s [33] DFT studies showed that proton transfer in hydrated adenine dimer ions can occur with negligible barriers. Kim et al. [22] discussed the possibility that proton transfer from water to adenine in the $n\pi^*$ excited state could explain the strong AH^+ production (as well as weak $A^+(H_2O)_n$ production) in their 266 nm MPI experiments. They concluded that this reaction was highly unlikely due to its large endothermicity in hydrated adenine. Hydrogen transfer from H_2O (homolytic bond cleavage energy 123 kcal/mol) to the adenine radical cation (H affinity 109 kcal/mol)

can also be ruled out [32]. Moreover, water is transparent at 220 nm [34] so AH[+] production in the present MPI experiments must begin with adenine excitation. The 136 Th peak may also contain a contribution of hypoxanthine[+] due to deamination reactions in closed-shell adenine-water complexes and subsequent cluster dissociation.

Notwithstanding the low laser fluence, Fig. 2 demonstrates significant fragment ion production in both dry and hydrated conditions. Table 1 lists the fragment ions that were clearly observed above the background level. Previous MPI-TOF measurements at 222 nm [25] have shown 28 Th products from laser-desorbed adenine in a supersonic jet. To our knowledge, the only other MPI fragment ion of adenine MPI mentioned in the literature is H^{+} (recorded at 266 nm with a much higher fluence than the present measurements [27]). Lin et al. [28] reported significant photo-dissociation of adenine in their 248 nm MPI experiments using ns-timescale laser pulses but did not specify the fragment ions. However dissociative ionisation of adenine has been studied extensively in ion impact [35 and references therein], electron impact [36], and single photon absorption [37] experiments. Taking into account differences in energy deposition and signal / noise ratios, the previous measurements were broadly consistent in terms of the fragment ions produced. Accordingly, Table 1 shows that the present dry adenine MPI mass spectrum includes all the strong fragment ions (>20% of the A[+] signal) observed in Jochims et al.'s [37] 20 eV photoionisation measurement. Only one weak peak is observed in the present dry adenine MPI result that has not been reported previously: 68 Th ($C_2H_2N_3^+$ or $C_3H_4N_2^+$), possibly indicating an unidentified excited state isomeric transition. On the basis of appearance energies and thermochemical data, Jochims et al. [37] proposed that the dominant fragmentation pathways of the excited adenine radical cation involve HCN loss followed by $C_4H_4N_4^+$ (108 Th with the lowest appearance energy) dissociation (notably via further HCN loss), CH_3N_2 loss followed by $C_2H_4N_3^+$ (70 Th) dissociation, and direct $C_4H_3N_4$ loss producing H_2CN^+ (28 Th).

The only previous studies of adenine dissociative ionisation in clusters were carried out on pure adenine complexes using MPI (266 nm ns-timescale laser pulses) [38] and 50 keV O_5^+ impact [39]. Schlathölter et al.'s ion impact experiments demonstrated strong production of 118 Th ions (indicating NH_3 loss, not observed in adenine monomers) as well as enhanced 119 Th (NH_2 loss) and 92 Th ($C_4H_2N_3^+$) signals due to clustering. The 119 and 109 Th fragment ions were most intense in Cheong et al.'s [38] MPI experiments on adenine clusters (minor peaks were mentioned but not listed); both strong photodissociation products of protonated adenine. The present work provides the first data on how clustering with water affects fragment ion production from adenine. Fig. 2 and Table 1 show that hydration significantly increased the count rate of 108 Th ($C_4H_4N_4^+$) ions as well as slightly enhancing 120 Th ($C_5H_4N_4^+$) and 119 Th ($C_5H_3N_4^+$) ion production. Conversely, it reduced the count rates of all the other fragment ions in the dry adenine MPI mass spectrum. These observations can be rationalised in terms of energy removal from the excited adenine cation via cluster dissociation tending to enhance the production of large fragment ions with low appearance energies at the expense smaller ions with relatively high appearance energies, predominantly associated with sequential fragmentation pathways. Hydration also opened a fragment ion channel at 18 Th (NH_4^+, discussed below).

Cheong et al. [38] analysed AH$^+$ fragmentation following photo-excitation at 266 and 263 nm (4.66 and 4.71 eV). In agreement with earlier collision induced dissociation (CID) experiments [40], the dominant fragment ions occurred at 119, 109 and 18 Th (see Table 1 for more detail). The hydrated adenine measurement in Fig. 2 (with enhanced 136 Th production), showed a clear increase in the 119 and 18 Th signals. The 119 Th fragment was also produced from dry adenine so its enhancement may be (wholly or partially) due to energy removal from the excited radical cation via water molecule loss limiting sequential fragmentation processes. Indeed, the absence of a clear peak at 109 Th in the hydrated adenine measurement suggests that AH$^+$ fragmentation did not contribute strongly to the present data. However the 18 Th signal in the hydrated adenine measurement provides compelling evidence for fragment ion production from AH$^+$. Our MPI experiments on argon-water beams did not produce any 18 Th ions, as expected considering water's transparency in the present wavelength range (220-225 nm) [34]. MPI (225 nm, average fluence 7×10^5 Wcm^{-2}) measurements on adenine (248°C) in an expansion with argon (0.9 bar) and D_2O (100°C) provided further evidence supporting the assignment of the present 18 Th peak to NH_4^+ production following AH$^+$ dissociation. Extensive hydrogen-deuterium exchange was evidenced by a series of peaks at 135-141 Th (maximum at 138 Th) replacing the 135 and 136 Th peaks observed in adenine-H_2O experiments. The mass spectrum also included a series of weak peaks between 18-22 Th, with a maximum at 21 Th indicating NHD_3^+ production.

Previous electron impact measurements [31] showed the strongest fragment ions derived from hypoxanthine to be at 54 and 28 Th (both also fragment ions from adenine, as shown in Table 1). Ion production at both of these m/q values was suppressed by hydration in the present data. Therefore the present data does not provide clear evidence for fragment ions traced to hypoxanthine formation in hydrated adenine complexes. This may be attributed to the fact that hypoxanthine is multi-photon ionised with much lower efficiency than adenine in the present laser fluence regime (Fig. 1), hence any fragment ion production will also be relatively weak. It is interesting to note that the total ion count rate in the hydrated measurement is only 21% of that in the dry measurement. There are a number of possible concurrent mechanisms that can reduce the total MPI signal. In MPI experiments using ns-timescale laser pulses at 266 nm, Nam et al. [21] observed that hydration increased the number of photons required for A$^+$ MPI production by one (hence reducing MPI efficiency at a given fluence) and attributed this to energy loss via cluster dissociation in the neutral electronic excited state. Hydration can also cause shifts in the excited states of nucleobases (notably stabilisation of nπ* states [41, 42]) and hence modify their relaxation dynamics with resultant changes in MPI efficiency.

3.3. Comparing MPI and EII of hydrated adenine complexes

Fig. 3 compares MPI and EII mass spectra of adenine-water clusters. As $A_2H^+(H_2O)_n$ peaks in the EII mass spectrum could not be separated from $(H_2O)_nH^+$ (n≥15), the present discussion focuses on the production of A$^+(H_2O)_n$ and $136^+(H_2O)_n$ (AH$^+(H_2O)_n$ or hydrated hypoxanthine complexes). EII

experiments on adenine-water clusters have been carried out by Kim et al. [22, 43]. However, whereas hydrated protonated thymine and uracil clusters were demonstrated, the presented mass spectra did not distinguish between $A^+(H_2O)_n$ and $136^+(H_2O)_n$. The EII plot in Fig. 3 shows a series of $136^+(H_2O)_n$ peaks preceded by weaker features attributed to $A^+(H_2O)_n$. As discussed above, AH^+ production in pure adenine clusters is attributed the proton transfer in adenine dimer ions followed by dissociation [11]. However this mechanism is very unlikely to produce $AH^+(H_2O)_n$ because complete loss of water molecules is expected to precede the cleavage of A_2^+ due to its high binding energy (e.g. 1.34 eV in $A_2^+(H_2O)$) compared with adenine-water (e.g. 0.49 eV in $A_2^+(H_2O)$) [44]. Alternatively, the removal of an electron from water in a hydrated cluster can lead to partial dissociation with a remaining excess proton (as observed for the pure protonated water clusters) that can migrate to adenine due to its markedly higher proton affinity [45]. While hypoxanthine formation may also contribute to the $136^+(H_2O)_n$ peaks (the calculated closed-shell deamination reaction barrier is only -2.4 kcal/mol [12] so little water molecule loss is expected), the fact that hydrated protonated thymine and adenine have been observed in Kim et al.'s [43] EII measurements indicates that water ionisation followed by dissociation and proton migration to adenine is highly likely to take place in the present EII experiments.

Previous mass spectra of adenine-water clusters have been measured using diverse MPI schemes with both ns-timescale and fs-timescale laser pulses [20, 21]. The novelty of the MPI mass spectrum in Fig. 3 is that it is presented in sufficient detail to reveal $136^+(H_2O)_n$ peaks. The production of these ions cannot be initiated by water ionisation at this wavelength [34]) and $AH^+(H_2O)_n$ formation via proton transfer in hydrated adenine dimer ions is very unlikely (see argument above). This leaves hypoxanthine$^+(H_2O)_n$ as the most probable assignment for the present $136^+(H_2O)_n$ MPI signals. Hence the high ratio of $136^+(H_2O)_n$ / $A^+(H_2O)_n$ counts in the EII measurement compared with the MPI data is consistent with the low MPI efficiency of hypoxanthine (Fig. 1) as well as the opening of the water ionisation induced proton transfer pathway in EII. Kim et al. [43] reported evidence for analogous hydrolytic deamination reactions in cytosine-water clusters.

The assignment of hypoxanthine$^+(H_2O)_n$ peaks in the present MPI mass spectrum has possible implications relevant to the structure of the adenine-water complexes in the neutral beam. The present data and previous mass spectra of adenine-water complexes [22] show evidence for $A^+(H_2O)_n$ production extending to at least n=7 and Kim et al.'s [24] calculations support a closed shell structure at n=4. Therefore deamination reactions in closed-shell adenine-water complexes could reasonably be expected lead to negligible production of large $A^+(H_2O)_n$ complexes. A possible explanation for $A^+(H_2O)_n$ production with n>4 is that a significant proportion of the $A(H_2O)_n$ complexes in the neutral beam do not have closed-shell configurations; water-water bonds have formed while at least one hydrogen-bonding site of adenine remains vacant. This interpretation appears to be broadly consistent with semi-empirical optimised structure calculations [46, 47] showing that water molecules preferentially group around a single bonding site in $A(H_2O)_n$ (n≤3). It is interesting to note that Liu et al. [48] reported significant hydration effects on the collision induced dissociation of adenosine

monophosphate anions (AMP$^-$) with up to 13 water molecules preferentially clustered on one side of the anion.

The MPI measurements revealed a broad peak centred at 193.7 Th. This feature is most likely due to the dissociation of excited cluster ions in the TOF drift tube. Kim at al. [24] also observed evidence for metastable dissociation of pure and hydrated adenine cluster ions, while Alvarado et al. [49] have shown that adenine cation fragmentation can proceed via CN loss followed by neutral H loss after a microsecond-order delay. Modelling ion flight times demonstrated that either A$^+$ or AH$^+$ formation by A$_2^+$ dissociation in the drift tube could produce the observed feature. Further experiments using the reflection voltage to determine the ion's kinetic energy are necessary to identify the fragmentation process unambiguously.

4. Conclusions

The present MPI and EII data enhances our understanding of the unimolecular and intermolecular reactive processes in adenine-water clusters. With the exception of the C$_5$H$_4$N$_4^+$, C$_5$H$_3$N$_4^+$, and C$_4$H$_4$N$_4^+$ fragment ion channels, clustering with water stabilised adenine with respect to dissociative ionisation. All sequential fragment ion pathways were suppressed. These hydration effects can be attributed to energy dissipation from the excited radical cation via cluster dissociation. Water ionisation followed by partial cluster dissociation and proton migration to adenine is expected to dominate 136$^+$(H$_2$O)$_n$ production in the present EII experiments. Weak 136$^+$(H$_2$O)$_n$ MPI peaks have been observed for the first time. MPI experiments on isolated hypoxanthine were carried out to verify whether the 136$^+$(H$_2$O)$_n$ peaks could be assigned to hydrated hypoxanthine ions following deamination reactions in closed-shell adenine water clusters. Accordingly, hypoxanthine was successfully ionised using ns-timescale laser pulses for the first time. The low MPI efficiency compared with adenine suggests particularly fast internal conversion to the electronic ground state following $\pi\pi^*$ excitation.

Acknowledgements

References

1) C. T. Middleton, K. de La Harpe, C. Su, Y.K. Law, C. E. Crespo-Hernandez, B. Kohler, Annu. Rev. Phys. Chem., 2009, **60**, 217.

2) N.L. Evans, S. Ullrich, *J. Phys. Chem. A*, 2010, **114**, 11225.

3) H. Kang, J. Chang, S.H. Lee, T.K. Ahn, N.J. Kim, S.K. Kim, *J. Chem. Phys*., 2010, **133**, 154311.

4) V.R. Smith, E. Samoylova, H.-H. Ritze, W. Radloff, T. Schultz, Phys. Chem. Chem. Phys., 2010, **12**, 9632.

5) H. Ritze, H. Lippert, E. Samoylova, V. Smith, I. Hertel, W. Radloff, T. Schultz, J. Chem. Phys., 2005, **122,** 224320.

6) L. Gonzalez-Luque, T. Climent, I. Gonzalez-Ramirez, M. Merchan, L. Serrano-Andres, *J. Chem. Theory Comput*., 2010, **6**, 2103.

7) R. Mitric, U. Werner, M. Wohlgemuth, G. Seifert and V. Bonacic-Koutecký, J. Phys. Chem. A, 2009, **113,** 12700.

8) S. Ullrich, T. Schultz, M.Z. Zgierski, A. Stolow, J. Am. Chem. Soc., 2004, **126**, 2262.

9) X. Chen, E.A. Syrstad, M.T. Nguyen, P. Gerbaux, F. Turecek, *J. Phys. Chem. A*, 2004, **108**, 9283.

10) Y. Nosenko, M. Kunitski, C. Riehn, P. H. Harbach, A. Dreuw and B. Brutschy, PCCP, 2010, **12,** 863.

11) I. Hünig, C. Plützer, K.A. Seefeld, D. Löwenich, M. Nispel, K. Kleinermanns, ChemPhysChem, 2004, **5**, 1427.

12) A.H. Zhang, B.H. Yang, Z.H. Li, Journal of Molecular Structure-Theochem., 2007, **819**, 95.

13) H.Y. Zheng, F.C. Meng, Structural Chemistry, 2009, **20**, 943.

14) L. R. Rutledge, C. A. Wheaton, S. D. Wetmore Physical Chemistry Chemical Physics, 2007, **9**, 497.

15) M. K. Shukla, J. Leszczynski, Journal of Physical Chemistry A, 2003, **107**, 5538.

16) X. J. Sun, J. K. Lee, Journal of Organic Chemistry, 2007, **72**, 6548.

17) B. Barc, M. Ryszka, J. Spurrell, M. Dampc, P. Limão-Vieira, R. Parajuli, N.J. Mason, S. Eden, J. Chem. Phys., 2013, **139**, 244311.

18) P. Colarusso, K. Zhang, B. Guo, P.F. Bernath, Chem. Phys. Lett., 1997, **269**, 39.

19) C. F. Guerra, F. M. Bickelhaupt, S. Saha, F. Wang, Journal of Physical Chemistry A., 2006, **110**, 4012.

20) M. Fernandez-Quejo, A. de la Fuente, R. Navarro, Journal of Molecular Structure., 2005, **744**, 749.

21) S.H. Nam, H.S. Park, J.K. Song, S.M. Park, J. Phys. Chem. A, 2007, **111**, 3480.

22) N.J. Kim, H. Kang, G. Jeong, Y.S. Kim, K.T. Lee, S.K. Kim, J. Phys. Chem. A, 2000, **104**, 6552.

23) N. Gador, E. Samoylova, V.R. Smith, A. Stolow, D.M. Rayner, W. Radloff, I.V. Hertel, T. Schultz, J. Phys. Chem. A, 2007, **11**, 11743.

24) N.J. Kim, Y.S. Kim, G. Jeong, T.K. Ahn, S.K. Kim, Int. J. Mass Spectrom., 2002, **219**, 11.

25) R. Tembreull, D.M. Lubman, Anal. Chem., 1987, **59**, 1082.

26) J.H. Hahn, R. Zenobi, R.N. Zare, J. Am. Chem. Soc., 1987, **109**, 2842.

27) K.L. Wells, G.M. Roberts, V.G. Stavros, Chem. Phys. Lett., 2007, **446**, 20.

28) C. Lin, J. Matsumoto, S. Ohtake, T. Imasaka, Talanta, 1996, **43**, 1925.

29) M.S. de Vries, Isolated DNA base Pairs, Interplay Between Theory and Experiment, in Radiation Induced Molecular Phenomena in Nucleic Acids, ed. M.K. Shukla, J. Leszczynski, 2008, Springer, Netherlands, 323.

30) P. Mozejko, L. Sanche, Radiation and Environmental Biophysics, 2003, **43**, 201.

31) NIST Chemistry WebBook, http//webbook.nist.gov, accessed 2013.

32) C.T. Hwang, C.L. Stumpf, Y.Q. Yu, H.I. Kenttamaa, Int. J. Mass Spectrom., 1999, **182**, 253.

33) H.S. Park, S.H Nam, J.K Song, S.M. Park, S. Ryu, J. Phys. Chem. A, 2008, **112**, 9023.

34) R. Mota, R. Parafita, A. Giuliani, M.-J. Hubin-Franskin, J.M.C. Lourenço, G. Garcia, S.V. Hoffmann, N.J. Mason, P.A. Ribeiro, M. Raposo, P. Limão-Vieira, Chem. Phys. Lett., 2005, **416**, 152.

35) J. Tabet, S. Eden, S. Feil, H. Abdoul-Carime, B. Farizon, M. Farizon, S. Ouaskit, T.D. Märk, Int. J. Mass Spectrom., 2010, **292**, 53.

36) J.M. Rice, G.O. Dudek, J. Am. Chem. Soc., 1967, **89**, 2719.

37) H.W. Jochims, M. Schwell, H. Baumgartel, S. Leach, Chem. Phys., 2005, **314**, 263.

38) N.R. Cheong, S.H. Nam, H.S. Park, S. Ryu, J.K. Song, S.M. Park, M. Perot, B. Lucas, M. Barat, J.A. Fayeton, C. Jouvet, Phys. Chem. Chem. Phys., 2011, **13**, 291.

39) T. Schlathölter, F. Alvarado, S. Bari, A. Lecointre, R. Hoekstra, V. Bernigaud, B. Manil, J. Rangama, B. Huber, ChemPhysChem, 2006, **7**, 2339.

40) C.C. Nelson, J.A. McCloskey, J. Am. Chem. Soc., 1992, **114**, 3661.

41) J.J. Szymczak, T. Müller, H. Lischka, Chem. Phys., 2010, **375**, 110.

42) L. Blancafort, A. Migani, J. Photochem. Photobiol. A - Chem., 2007, **190**, 283.

43) S. K. Kim, W. Lee, D. R. Herschbach, Journal of Physical Chemistry, 1996, **100**, 7933.

44) S.H. Nam, H.S. Park, S. Ryu, J.K. Song, S.M. Park, Chem. Phys. Lett., 2008, **450**, 236.

45) M. Meot-Ner, J. Am. Chem. Soc., 1979, **101**, 2396.

46) S. Carles, C.F. Lecomte, J.P. Schermann, C. Desfrancois, *J. Phys. Chem. A*, 2000, **104**, 10662.

47) V. Periquet, A. Moreau, S. Carles, J.P. Schermann, C. Desfrancois, Journal of Electron Spectroscopy and Related Phenomena, 2000, **106**, 141.

48) B. Liu, S. Brøndsted Nielsen, P. Hvelplund, H. Zettergren, H. Cederquist, B. Manil, B.A. Huber, Phys. Rev. Lett., 2006, **97**, 133401.

49) F. Alvarado, S. Bari, R. Hoekstra, T. Schlathölter, J. Chem. Phys., 2007, **127**, 034301

Figure 1: Comparison of MPI (220 nm, average fluence 4×10^7 Wcm^{-2}) and EII (200 eV) of adenine and hypoxanthine (Ar 0.5 bar). The most abundant gas-phase tautomers (amine-N9H adenine [19] and keto-N1H/N9H hypoxanthine [20]) are shown on the right.
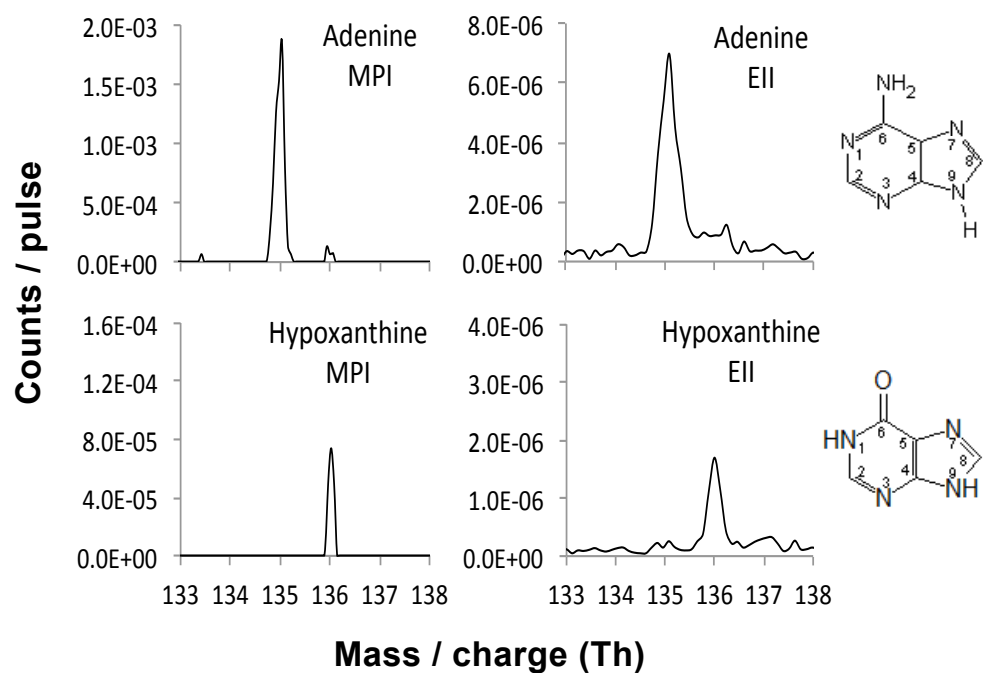
Figure 2: MPI mass spectra (225 nm, average fluence 4×10^5 Wcm^{-2}, powder 237°C, Ar 0.8 bar) of dry adenine and hydrated adenine (water 100°C).

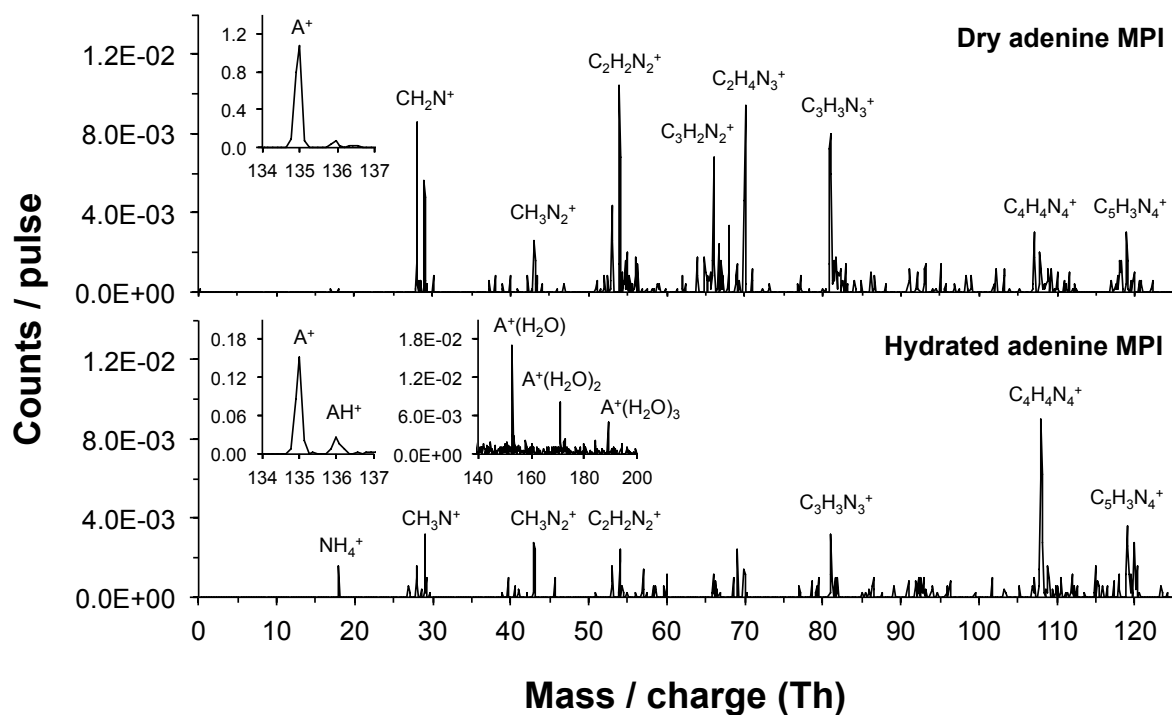**Figure 3:** Comparison of MPI (upper plot, 220 nm, average fluence 3×10^6 Wcm^{-2}) and EII (lower plot, 200 eV) mass spectra of hydrated adenine (powder 276°C, water 70°C, Ar 1.8 bar).
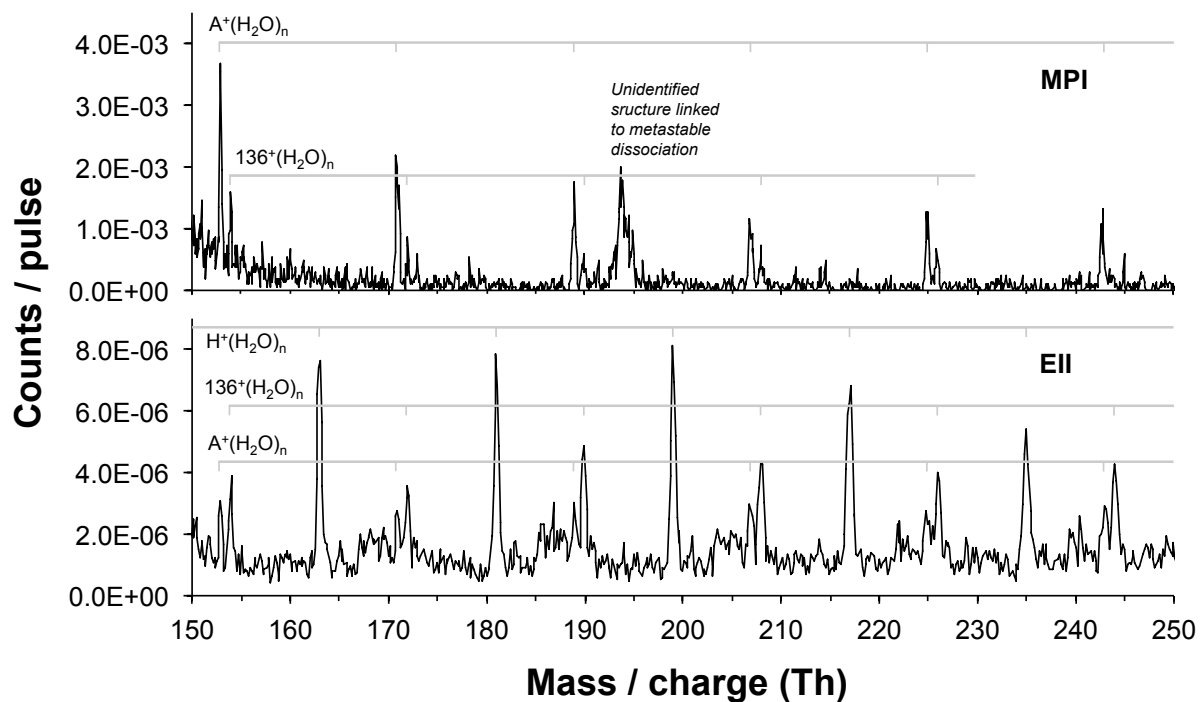
Table 1: Ions observed following MPI of adenine in dry and hydrated conditions (Fig. 2 data, not including cluster ions), photoionisation (20 eV) of adenine [37], photo-dissociation of protonated adenine (266 nm, average fluence ~10^7 Wcm^{-2}) [38], and EII (electron energy not available) of hypoxanthine [31].

m/q (Th)	% of the parent ion peak (except in the case of AH$^+$) with the previously proposed assignments, where available.				
	Adenine MPI [A]	Hydrated adenine MPI [A]	Adenine photoionisation [37]	AH$^+$ photo-dissociation [38] [B]	Hypoxanthine EII [31] [B]
136	8.0 ±0.4	23 ±2	*Not shown*	*Not shown*	100
135	100	100	100 ($C_5H_5N_5^+$)	*Not shown*	10
134	0.3 ±0.1	0.8 ±0.3	10 ($C_5H_4N_5^+$)	*Not shown*	
120	**0.08 ±0.04**	**1.2 ±0.4**	**1 ($C_5H_4N_4^+$)**		
119	**0.3 ±0.1**	**3.3 ±0.6**	**3 ($C_5H_3N_4^+$)**	**100 ($C_5H_3N_4^+$)**	
109				31 ($C_4H_5N_4^+$)	10
108	**0.2 ±0.1**	**10 ±1**	**57 ($C_4H_4N_4^+$)**		**10**
107	0.3 ±0.1	0.7 ±0.3	10 ($C_4H_3N_4^+$)		
94				13 ($C_4H_4N_3^+$)	
92			9 ($C_4H_2N_3^+$)		
82				5 ($C_3H_4N_3^+$)	
81	1.2 ±0.2	2.3 ±0.5	50 ($C_3H_3N_3^+$)		10
80			10 ($C_3H_2N_3^+$)		3
70	0.7 ±0.1	1.0 ±0.3	17 ($C_2H_4N_3^+$)		1
68	0.2 ±0.1				1
67			10 ($C_3H_3N_2^+$)	5 ($C_3H_3N_2^+$)	1
66	0.8 ±0.1	0.6 ±0.3	41 ($C_3H_2N_2^+$)		3
65					1
55				5 ($C_2H_3N_2^+$)	
54	0.9 ±0.1	1.6 ±0.4	55 ($C_2H_2N_2^+$)		30
53	0.4 ±0.1	1.1 ±0.4	28 ($C_2HN_2^+$)		8
43	0.3 ±0.1	2.0 ±0.5	34 ($CH_3N_2^+$)		2
42			16 ($CH_3N_2^+$)		
41			7 (CHN_2^+)		
40			1 (CN_2^+)		
39			1 (C_2HN^+)		3
38					3
29	0.6 ±0.1	1.4 ±0.4	60 (CH_3N^+)		7
28	0.7 ±0.1	1.3 ±0.4	110 (CH_2N^+)	5 (CH_2N^+)	32
27			10 (CHN^+)		4
18		**0.6 ±0.3**	***Not shown***	**25 (NH_4^+)**	

Fragment ion peaks that have higher MPI count rates in the hydrated measurement than in the dry measurement are highlighted in bold.
[A] The MPI columns only include peaks with count rates that are clearly greater than background measurements. The error boundaries are based on assumed Poisson statistics.
[B] The approximate percentages in the AH$^+$ photo-dissociation and hypoxanthine EII columns were read from figures. Trace features in the mass spectra are not included.